Tellus (1999), 51A, 337–348
Printed in UK – all rights reserved

TELLUS
ISSN 0280–6495

Numerical solutions of the vertical structure equation and associated energetics

By J. M. CASTANHEIRA[1]*, C. C. DaCAMARA[2] and A. ROCHA[3], [1,3]*Department of Physics, University of Aveiro, 3810 Aveiro, Portugal;* [2]*Department of Physics, University of Lisbon, 1700 Lisbon, Portugal*

(Manuscript received 28 July 1998; in final form 4 December 1998)

ABSTRACT

The vertical structure equation (VSE) is solved by a Galerkin method as used by Kasahara. The sensitivity of the vertical decomposition to the truncation order of the Legendre polynomials series is studied, with the aim of finding an adequate truncation order for a given data set. Obtained results show that: (1) the vertical scale decomposition presents little sensitivity to the truncation order; (2) the order of truncation may be greater than the number of discrete levels in the data set. It is finally shown that the proposed choice of truncation order may overcome the problem of aliasing in the higher internal modes.

1. Introduction

The orthogonal projection of the atmospheric circulation field onto 3-dimensional normal mode functions (3-D NMFs), as introduced by Kasahara and Puri (1981), allows partitioning the circulation field into gravity and rotational components, a feature that makes of normal modes an important tool, both in objective data analysis and in model initialization (Daley, 1991).

Global energetics analysis using 3-D NMFs as a base (Kasahara and Puri, 1981; Tanaka, 1985; Tanaka and Kung, 1988) lays the grounds for a unified frame encompassing the three, 1-dimensional spectral energetics, respectively, in the zonal, meridional and vertical domains. On the other hand, the normal mode energetics scheme yields a 3-dimensional spatial scale separation of horizontal motion and mass fields, and allows an energy partition between barotropic and baroclinic components on the one hand, and Rossby and gravity waves on the other.

* Corresponding author.
e-mail: jcast@fis.ua.pt

The problem involves solving a linearized system of primitive equations with the aim of building up an orthogonal base of functions, and is therefore a problem of free oscillations. Using the vertical transform (Fulton and Schubert, 1985) or the standard method of separation of variables yields separate equations for the horizontal and vertical structures, which are related by a separation constant, the inverse of equivalent depth. The vertical structure equation (VSE) together with appropriate model boundary conditions constitute a Sturm–Liouville eigenvalue problem, which is first solved in order to obtain vertical structure functions (VSFs) and associated equivalent depths. Substitution of the equivalent depth into the horizontal structure equations (HSEs) allows for the determination of the horizontal structure functions (HSFs), which are obtained as eigenvectors of a horizontal operator, the associated eigenvalues being the frequencies of oscillation.

In this scheme, although the dispersive characteristics are explicitly present on the horizontal structure, they are closely related to the vertical structure by the vertical depth spectrum. Since the temporal scales of the HSFs depend on the equiva-

lent depth, they are associated with, the dispersive characteristics of a given data set, when projected onto a normal mode base, may therefore be biased by the vertical partition of energy.

Analytic solutions of the VSE are only available for special forms of the vertical temperature profile (Staniforth et al., 1985), and therefore, in practical cases, the equation has to be solved using numerical methods: finite-differences (Kasahara and Puri, 1981), finite-elements (Daley, 1978) and spectral methods (Kasahara, 1984; Fulton and Schubert, 1985).

Several studies have examined the accuracy of different numerical methods comparing numerical and analytic solutions calculated for certain specific stability parameters (Staniforth et al., 1985; Sasaki and Chang, 1985; Fulton and Schubert, 1985). In this paper, the VSE is numerically solved with a Galerkin method as used by Kasahara (1984). The main purpose is to assess the sensitivity of the vertical partition of energy (vertical energy spectrum) to the order of truncation of the series of Legendre polynomials, and then establish a criterion allowing us to determine an appropriate order of truncation for a given data set. It is worth noting that this problem has to be addressed, both in diagnostic and in temporal evolution studies, in order to understand the effect of a particular normal base choice on the dispersive properties of the data.

A linearized primitive equation model and the method to construct the VSFs will be described in Section 2. Section 3 will present the simple analytic case of an isothermal atmosphere with a rigid lid at the top $p_t \neq 0$. The representation of an analytic spectrum on vertical numeric mode bases, calculated for different truncation orders of the series of Legendre polynomials, will be investigated. The vertical normal mode energetics of the FGGE IIIb and the NCEP (National Centers for Environmental Prediction) atmospheres, for the period of 16–31 January 1979, will be examined in Section 4. In Subsection 4.1, the FGGE IIIb atmospheric spectra of eddy kinectic and eddy available potential energies will be calculated for different numeric vertical bases, using the same procedure as in Section 3. In Subsection 4.2, an assessment is made of the effects of vertical resolution of the data set, using the NCEP re-analyses. Finally, Section 5 summarizes the main results that were obtained.

2. Theory

2.1. A linearized tridimensional model

The set of primitive equations of an hydrostatic and adiabatic atmosphere, linearized with respect to a basic state at rest having a pressure dependent temperature distribution T_0, may be written in the following form:

$$\begin{aligned} &\frac{\partial \mu}{\partial t} - 2\Omega v \sin\theta + \frac{1}{a\cos\theta}\frac{\partial \phi}{\partial \lambda} = 0, \\ &\frac{\partial v}{\partial t} + 2\Omega u \sin\theta + \frac{1}{a}\frac{\partial \phi}{\partial \theta} = 0, \\ &\frac{\partial}{\partial t}\frac{\partial}{\partial p}\left(\frac{1}{S_0}\frac{\partial \phi}{\partial p}\right) - \nabla\cdot\dot{\boldsymbol{V}} = 0, \end{aligned} \tag{1}$$

where (λ, θ, p) are the longitude, latitude and pressure coordinates; ϕ is the perturbed field of geopotential and

$$S_0 = \frac{R}{p}\left(\frac{kT_0}{p} - \frac{\mathrm{d}T_0}{\mathrm{d}p}\right) \tag{2}$$

is the static stability parameter of the reference state. The remaining symbols in eqs. (1) and (2) are the horizontal wind components (u, v), the earth's radius a, the angular speed of the earth's rotation Ω, the specific gas constant R, and the ratio k of specific gas constant to specific heat at constant pressure.

As model boundary conditions, it will be assumed that $\omega = \mathrm{d}p/\mathrm{d}t$ vanishes as $p \to 0$ and that the linearized geometric vertical velocity $w = \mathrm{d}z/\mathrm{d}t$ vanishes at a constant pressure, p_s, near the earth's surface.

Performing the following separation of variables on eqs. (1)

$$\begin{bmatrix} u(\lambda,\theta,p,t) \\ v(\lambda,\theta,p,t) \\ \phi(\lambda,\theta,p,t) \end{bmatrix} = G(p) \begin{bmatrix} \hat{u}(\lambda,\theta,t) \\ \hat{v}(\lambda,\theta,t) \\ \hat{\phi}(\lambda,\theta,t) \end{bmatrix}, \tag{3}$$

one obtains the VSE

$$\frac{\mathrm{d}}{\mathrm{d}p}\left(\frac{1}{S_0}\frac{\mathrm{d}G}{\mathrm{d}p}\right) + \frac{G}{gh} = 0, \tag{4}$$

as well as the system of equations

$$\frac{\partial \hat{u}}{\partial t} - 2\Omega\hat{v}\sin\theta + \frac{1}{a\cos\theta}\frac{\partial \hat{\phi}}{\partial \lambda} = 0,$$

$$\frac{\partial \hat{v}}{\partial t} + 2\Omega\hat{u}\sin\theta + \frac{1}{a}\frac{\partial \hat{\phi}}{\partial \theta} = 0, \tag{5}$$

$$\frac{\partial \hat{\phi}}{\partial t} + \frac{gh}{a\cos\theta}\left[\frac{\partial \hat{u}}{\partial \lambda} + \frac{\partial(\hat{v}\cos\theta)}{\partial\theta}\right] = 0,$$

which determines the horizontal structure. In eqs. (4) and (5), the coefficient $-1/(gh)$ is the separation constant and h the equivalent depth.

Performing the same variable substitution on boundary conditions leads to

$$\frac{1}{S_0}\frac{\mathrm{d}G}{\mathrm{d}p} = 0, \qquad \text{as } p \to 0,$$

$$\frac{1}{S_0}\frac{\mathrm{d}G}{\mathrm{d}p} + \frac{p}{RT_0}G = 0, \qquad \text{at } p = p_\mathrm{s}. \tag{6}$$

2.2. *Solutions of the vertical structure equation*

As already mentioned, analytic solutions of eq. (4) are only possible for special forms of the stability parameter S_0. In this work, solutions of eq. (4) satisfying the boundary conditions (6) are numerically obtained with a Galerkin method as used by Kasahara (1984). For purposes of reference, a quick description of the method is given below.

Defining a new vertical coordinate

$$\sigma = 2\frac{p}{p_\mathrm{s}} - 1, \tag{7}$$

the VSE (4) may be rewritten as

$$\frac{\mathrm{d}}{\mathrm{d}\sigma}\left[\frac{(1+\sigma)}{\Gamma_0}\frac{\mathrm{d}G}{\mathrm{d}\sigma}\right] + \eta G = 0, \tag{8}$$

where $\eta = R/gh$, and Γ_0 is the static stability parameter in the new coordinate σ, defined as

$$\Gamma_0 = \frac{kT_0}{1+\sigma} - \frac{\mathrm{d}T_0}{\mathrm{d}\sigma}. \tag{9}$$

Parameters S_0 and Γ_0 are related by the equation

$$\frac{\Gamma_0}{1+\sigma} = \frac{p_\mathrm{s}^2}{4R}S_0. \tag{10}$$

Introducing the vertical coordinate σ on the boundary conditions (6) one obtains

$$\frac{1+\sigma}{\Gamma_0}\frac{\mathrm{d}G}{\mathrm{d}\sigma} = 0, \qquad \text{as } \sigma \to -1,$$

$$\frac{\mathrm{d}G}{\mathrm{d}\sigma} + \frac{\Gamma_0}{T_0}G = 0, \qquad \text{at } \sigma = 1. \tag{11}$$

Solutions of eq. (8) are then approximated by a series expansion

$$G_n^a(\sigma) = \sum_{j=0}^{N-1} a_j^n P_j(\sigma), \tag{12}$$

where $P_j(\sigma)$ are Legendre polynomials which satisfy to the orthonormality condition

$$\int_{-1}^{1} P_i(\sigma)P_j(\sigma)\,\mathrm{d}\sigma = \delta_{ij}. \tag{13}$$

Expansion coefficients a_j^n in (12) are calculated by the Galerkin method, i.e.,

$$\int_{-1}^{1}\left\{\frac{\mathrm{d}}{\mathrm{d}\sigma}\left[\frac{1+\sigma}{\Gamma_0}\frac{\mathrm{d}G}{\mathrm{d}\sigma}\right] + \eta G\right\}P_i\,\mathrm{d}\sigma = 0,$$

$$i = 0, \ldots, N-1. \tag{14}$$

Calculating the above integral by parts, substituting boundary conditions (11) and applying the orthonormality condition (13) one obtains the following matrix equation

$$\mathbf{M}\boldsymbol{X}_n = \eta\boldsymbol{X}_n, \tag{15}$$

where $\boldsymbol{X}_n = (a_0^n, \ldots, a_{N-1}^n)^\mathrm{T}$ and $\mathbf{M}$ is a symmetric matrix whose elements are given by

$$m_{ij} = \int_{-1}^{1}\frac{1+\sigma}{\Gamma_0}\frac{\mathrm{d}P_i}{\mathrm{d}\sigma}\frac{\mathrm{d}P_j}{\mathrm{d}\sigma}\,\mathrm{d}\sigma + \left[\frac{2}{T_0}P_iP_j\right]_{\sigma=1}. \tag{16}$$

Since $\mathbf{M}$ is a symmetric matrix, eigenvectors associated with different eigenvalues are orthogonal. The orthonormality condition is

$$\sum_{j=0}^{N-1} a_j^m a_j^n = \delta_{mn}. \tag{17}$$

Taking into account relations (17) and (13), it is easy to verify that the approximate solutions G_n^a satisfy the orthonormality condition

$$\int_{-1}^{1} G_m^a(\sigma)G_n^a(\sigma)\,\mathrm{d}\sigma = \delta_{mn}. \tag{18}$$

Finally, using the pressure coordinate, eq. (18) takes the form

$$\frac{2}{p_s}\int_0^{p_\mathrm{s}} G_m^a(p)G_n^a(p)\,\mathrm{d}p = \delta_{mn}. \tag{19}$$

2.3. Vertical mode decomposition

The vertical profile of the vector $(u, v, \phi)^{\mathrm{T}}$ may be decomposed into a series of VSFs, G_m^a:

$$(u, v, \phi)^{\mathrm{T}} = \sum_{j=0}^{N-1} \tilde{\boldsymbol{W}}_j(\lambda, \theta, t) G_j^a(p) \tag{20}$$

with vectors $\boldsymbol{W}_j = (\hat{u}_j, \hat{v}_j, \hat{\phi}_j)^{\mathrm{T}}$ given by

$$\boldsymbol{W}_j(\lambda, \theta, t) = \frac{2}{p_{\mathrm{s}}} \int_0^{p_{\mathrm{s}}} (u, v, \phi)^{\mathrm{T}} G_j^a(p)\, \mathrm{d}p. \tag{21}$$

The kinetic energy K_m and the available potential energy P_m per unit square of horizontal area, associated with each vertical mode m, are given by

$$K_m = \frac{p_{\mathrm{s}}}{2g} \frac{1}{4\pi} \int_0^{2\pi} \int_{-\pi/2}^{\pi/2} \frac{\hat{u}_m^2 + \hat{v}_m^2}{2} \cos\theta\, \mathrm{d}\theta\, \mathrm{d}\lambda, \tag{22}$$

$$P_m = \frac{p_{\mathrm{s}}}{2g} \frac{1}{4\pi} \int_0^{2\pi} \int_{-\pi/2}^{\pi/2} \frac{\hat{\phi}_m^2}{2gh_{\mathrm{m}}} \cos\theta\, \mathrm{d}\theta\, \mathrm{d}\lambda. \tag{23}$$

It is worth noting that integrations in eqs. (16) and (21) were performed through Gaussian quadrature, implying a redefinition of the inner product as

$$(f, g) = \sum_{i=1}^{N_{\mathrm{A}}} w_i f_i g_i, \tag{24}$$

where w_i are the weights, f_i and g_i the function values at Gaussian levels and N_{A} the number of levels. If $N_{\mathrm{A}} \geqslant N$ integration (13) will be exactly computed by Gaussian quadrature and the orthonormality of the VSFs (12) will be kept in the new definition of the inner product (24). In this work the value of N_{A} was chosen to be $N_{\mathrm{A}} = N + 20$.

3. Isothermal atmosphere

In order to assess the sensitivity of the vertical partition of energy, as a function of the equivalent depth, to the number of Legendre polynomials, N, used in the calculation of G_m^a, an heuristic procedure is followed. First, some computational experiments were performed on an isothermal atmosphere, $T = 250$ K, with a rigid lid at the top, $p_{\mathrm{t}} = 4.3$ hPa.

In this model of the atmosphere, the linearized version of the geometric velocity $w = \mathrm{d}z/\mathrm{d}t$ vanishes both at the bottom and at the top. The VSFs may be analytically calculated and constitute a discrete base (Daley, 1991), with the barotropic mode ($m = 0$) given by

$$G_0(p) = \left(\frac{p}{p_{\mathrm{s}}}\right)^{-k}, \tag{25}$$

and the baroclinic modes ($m \geqslant 1$) by:

$$G_m(p) = \sqrt{\frac{p_{\mathrm{s}}}{p}} \left[\cos \frac{m\pi \ln(p_{\mathrm{s}}/p)}{\ln(p_s/p_{\mathrm{t}})} + \frac{\ln(p_{\mathrm{s}}/p_{\mathrm{t}})(k - 1/2)}{m\pi} \times \sin \frac{m\pi \ln(p_{\mathrm{s}}/p)}{\ln(p_{\mathrm{s}}/p_{\mathrm{t}})} \right]. \tag{26}$$

The equivalent depths of the barotropic mode and baroclinic modes are respectively given by

$$h_0 = \frac{RT}{g(1-k)}, \tag{27}$$

$$h_m = \frac{4RkT \ln^2(p_{\mathrm{s}}/p_{\mathrm{t}})}{g[\ln^2(p_{\mathrm{s}}/p_{\mathrm{t}}) + 4m^2\pi^2]}. \tag{28}$$

The VSFs have also been computed numerically by the method described in Subsection 2.2. Fig. 1 shows the ratio of numeric to analytic equivalent depths of the modes = 0, 5, 10, 15, 19 as a function of N, allowing to estimate the rate of convergence of the numerical method; it is worth noting that the numeric equivalent depths of the first 20 modes, calculated with 100 Legendre polynomials, have an error smaller than 0.6%.

Fig. 2 presents an example of an analytic vertical profile of a perturbed field of geopotential given

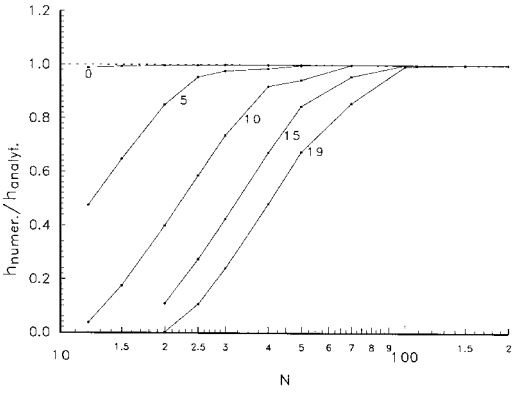

Fig. 1. Ratio of numeric to analytic equivalent depths of the modes 0, 5, 10, 15 and 19, as a function of N.

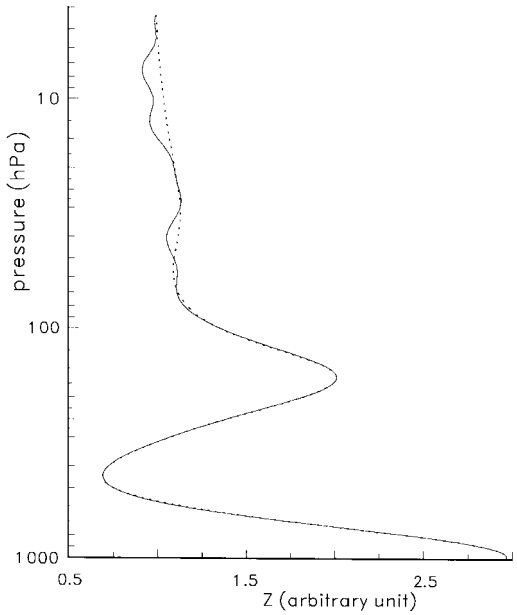

Fig. 2. Vertical profile of analytic (solid line) and interpolated (dashed line) perturbed field of geopotential.

by a linear combination of the first 20 analytic modes. Expansion coefficients were chosen with the aim of obtaining a vertical available potential energy spectrum similar to the one of FGGE data, to be analyzed in the next section, with maxima located at equivalent depths of the same order of magnitude. The analytic spectrum of available potential energy is represented in Fig. 3 by the plus sign symbols in the solid curve. The spectrum was computed using eq. (23) with the vertical geopotential profile (shown in Fig. 2) representing the mean value of the perturbed field of geopotential on isobaric surfaces.

The analytic perturbed field of geopotential was calculated for 12 standard isobaric levels (the same as those of FGGE-IIIb data considered in the next section: 1000, 850, 700, 500, 400, 300, 250, 200, 150, 100, 50 and 30 hPa), and at the top, p_t, and bottom, p_s, surfaces. These values were taken as "data", and were previously interpolated to the Gaussian levels by cubic splines (Fig. 2), and then projected onto the numeric modes using the definition (24) for the inner product.

Table 1 lists the sum of available potential energy contained in numeric modes with equivalent depths $h \geqslant 15$ m (the minimum equivalent depth of the analytic spectrum is 17 m), for different truncation orders N. The values in the table are approximately constant, with fluctuations smaller than 0.4%. It is worth noting that the maximum difference between the sum of the energy of numeric modes and the one of analytic modes is 1.1% of the latter.

The total available potential energy projected onto numeric modes with $h < 15$ m, expressed as a percentage of the total analytic energy, is shown in Table 2. One may observe that this value is appreciable only for the case $N = 12$, a fast decrease being observed for greater values of N. This behaviour may be explained by the formula utilized to calculate the available potential energy, where h appears in the denominator (eq. (23)): in fact, if the equivalent depths of the higher order internal modes are underestimated, then the available potential energy contained in those modes may be overestimated (Staniforth et al., 1985).

Fig. 3 also shows numeric spectra of available potential energy calculated for different values of N. Only those modes whose equivalent depth is greater than 15 m are represented. The global features of the analytic spectrum are reproduced by the numeric spectra, with the minima and maxima appearing, respectively, for the same vertical scales. The numeric modes present higher energy values than those of the analytic modes. This agrees to the fact that the total energy of the

Table 1. *Total available potential energy contained in vertical modes with $h \geqslant 15$ m*

N	12	15	25	40	50	70	100	200	Analyt.
M	9	10	13	17	18	19	21	21	20
$\sum_{m<M} P_m$	566.7	565.1	567.0	567.1	567.1	567.0	567.1	567.1	571.4

N is the number of Legendre polynomials used in the calculation of numeric modes. M is the number of modes with $h \geqslant 15$ m. Arbitrary units.

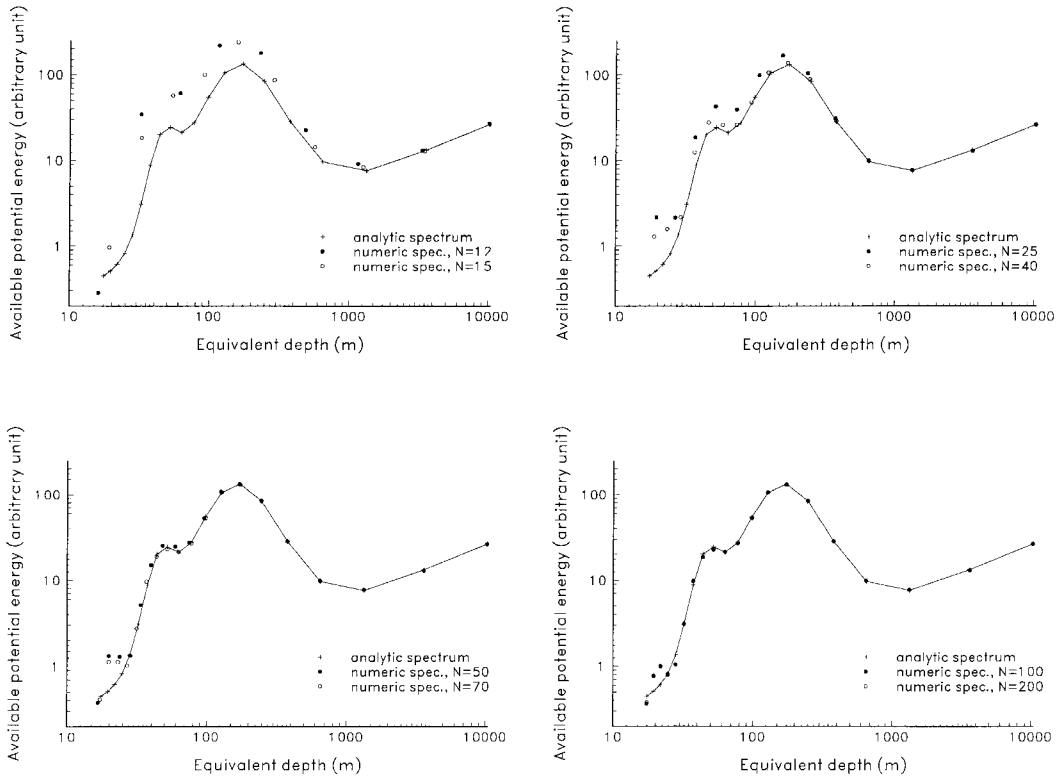

Fig. 3. Analytic (plus signs in the solid line) and numeric (empty and solid circles) energy spectra for different orders of truncation N.

Table 2. *Total available potential energy contained in numeric modes with $h < 15$ m, expressed as a % of total analytic energy*

N	12	15	25	40	50	70	100	200
$\sum_{m \geqslant M} P_m$ (%)	14.6	1.2	0.4	<0.1	<0.1	<0.1	<0.1	<0.1

N is the number of Legendre polynomials used in the calculation of numeric modes. M is the number of modes with $h \geqslant 15$ m. Arbitrary units.

numeric modes is approximately equal to the total energy of the analytic modes, whereas the number of numeric mode with $h \geqslant 15$ m is smaller than the number (20) of analytic modes. In other words, when the numeric spectra have lower resolution (i.e., when the vertical structure of the geopotential is resolved with a small number of modes), the energy of the numeric modes is larger than the energy of the analytic modes, each numeric mode receiving contributions from the neighbouring analytic modes.

It is worth noting that for $N = 15$, the points representing the energy of the barotropic mode on the numeric and analytic spectra are superposed. When $N = 25$, the superposition extends to the first three baroclinic modes, and for higher values of N more and more modes are coincident. However, this convergence process seems to stop at $N = 100$, but the reason for this apparent convergence saturation is to be attributed to the fact that the "observed" geopotential profile (Fig. 2), retrieved by cubic splines, does not

adequately reproduce the analytic geopotential in the upper atmosphere.

Recovery of the perturbed field of geopotential from "data" is a problem of the type of objective data analysis. If the 'observations' are adjusted to a linear combination of numeric modes, i.e.,

$$Z(p) = \sum_{m=0}^{M-1} c_m G_m(p) \tag{29}$$

by a least square minimization procedure, then the number M of modes in the expansion must be less or equal to the number of "observations", in order to guarantee a unique set of c_m coefficients.

Such c_m coefficients in (29) may also be calculated by interpolation of $Z(p)$, and inner multiplication of the interpolated function by $G_m(p)$ using definition (24). It is obvious that the interpolated function cannot contain more information than the discrete "data" and therefore the number of calculated c_m coefficients must be less or equal to the number of "observations".

Amongst the set of numeric bases, the appropriate one to project the "data" is the base that better adjusts to the analytic spectrum and explains the vertical variance (total energy) with M less or equal to the number of "observations". It must be emphasized that it is not N but the number M which determines the choice of the base. Therefore, as shown in Table 1, the first 13 ($M = 13$) modes calculated with 25 polynomials ($N = 25$) do constitute the appropriate base to project the simulated "data".

4. FGGE IIIb and NCEP atmospheres

4.1. FGGE IIIb analyses

An assessment of the sensitivity of the vertical partition of energy to the choice of a numeric vertical mode base using observed data, was performed using the Geophysical Fluid Dynamics Laboratory (GFDL) version of the FGGE IIIb data (twice daily at 0000 and 1200 UT) for the period 16–31 January 1979. The original GFDL analysis data at 1000, 850, 750, 500, 400, 300, 250, 200, 150, 100, 50 and 30 hPa, on a $1.875^\circ \times 1.875^\circ$ grid were interpolated to a $4^\circ \times 5^\circ$ grid with 46 latitudes from 90°S to 90°N and 72 longitudes from 0 to 355°E, as described by Kung and Tanaka (1983).

The global mean temperature of FGGE data was averaged for one year from 1 December 1978 through 30 November 1979 in order to define the basic state temperature $T_0(p)$. This basic state temperature was interpolated onto the Gaussian levels up to 30 hPa, the standard atmosphere being used above this level (Tanaka and Kung, 1989). The vertical derivative in eq. (2) was calculated by Taylor's series expansion of $T_0(p)$, the 4th and higher terms being neglected (Murakami, 1967). The zonal and meridional wind components and the perturbed field of geopotential were interpolated onto the Gaussian levels assuming $\boldsymbol{V} = 0$ at the surface. Above the 30 hPa level, $\boldsymbol{V}$ and ϕ were assumed to be constant and equal to their respective values at that level.

Vertical spectra of the eddy components of kinetic and available potential energies were calculated using different vertical mode bases, as described in Section 3, but with the static stability parameter of the FGGE atmosphere and boundary conditions (6). As remarked in Section 3, the total energy contained in numeric modes with equivalent depths greater than a specified minimum value, is approximately constant and independent of the considered number of modes. In the other hand, it was also referred that an underestimation of equivalent depths may result on an overestimation of the available potential energy. Taking these facts into account, a minimum value, $h_{\min}$, was defined for the equivalent depth, following the procedure described below.

First, the kinetic energy K and available potential energy P were directly computed from the data performing the following integrations

$$K = \frac{1}{2g}\frac{1}{4\pi}\int_0^{2\pi}\int_{-\pi/2}^{\pi/2}\int_0^{p_s}(u^2+v^2)\,\mathrm{d}p\cos\theta\,\mathrm{d}\theta\,\mathrm{d}\lambda, \tag{30}$$

$$P = \frac{1}{2g}\frac{1}{4\pi}\int_0^{2\pi}\int_{-\pi/2}^{\pi/2}\int_0^{p_s}\frac{1}{S_0}\left(\frac{\partial\phi}{\partial p}\right)^2\mathrm{d}p\cos\theta\,\mathrm{d}\theta\,\mathrm{d}\lambda. \tag{31}$$

The data were then projected onto the numeric bases looking for a value $h_{\min}$ such that the total kinetic energy and the total available potential energy, contained in numeric modes with $h \geqslant h_{\min}$, presented values close to those given by eqs. (30) and (31), independently of the number of modes. Vertical integrations in (30) and (31) were performed by Gaussian quadrature with $N_A = 36$, and the chosen minimum value was $h_{\min} = 2$ m.

Table 3 shows the total eddy kinetic energy and total eddy available potential energy calculated for different values of N, only including the modes with $h \geqslant 2$ m. Also shown are the values obtained by the direct integrations of eqs. (30) and (31).

It is worth mentioning that in the case $N = 12$, the available potential and kinetic energies contained in modes $m = 10$ and $m = 11$ with equivalent depths $h < 2$ m (therefore not included in Table 3) are 220.8 kJ m^{-2} and 1.6 kJ m^{-2}, respectively. These values represent 36% and 0.2% of the corresponding energies contained into the modes with $h \geqslant 2$ m, respectively. The obtained high value of available potential energy contained in modes $m = 10$ and $m = 11$ may be attributed to aliasing, arising from an underestimation of their equivalent depths, as explained in Section 3.

Figs. 4, 5 show the spectra of the eddy kinetic energy and eddy available potential energy calculated for different truncation orders N, respectively. Only the modes with $h \geqslant 2$ m are represented. As already explained in Section 3, the

Table 3. *Total eddy kinetic energy and total eddy available potential energy contained in numeric vertical modes with $h \geqslant 2$ m*

N	M	$\sum_{m<M} P_m$	$\sum_{m<M} K_m$
12	10	611.0	702.8
16	13	596.9	711.7
30	18	598.1	718.4
50	25	597.6	718.8
100	36	596.6	717.7
150	44	597.2	718.2
200	50	597.3	718.1
250	55	597.7	718.0
300	59	597.9	718.1
350	62	597.6	718.1
eqs. (30) and (31)		593.0	717.1

N is the number of Legendre polynomials used to calculate the numeric modes. M is the number of modes with $h \geqslant 2$ m. Units are kJ m^{-2}.

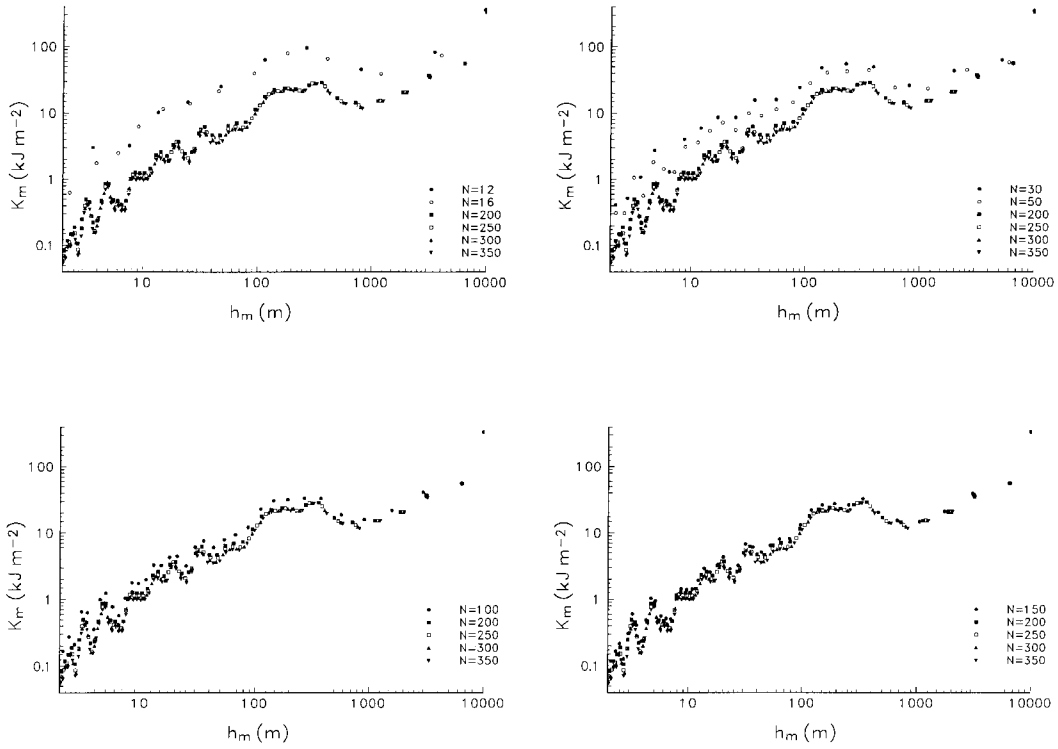

Fig. 4. Eddy kinetic energy spectra for the period 16–31 January 1979, for different truncation orders N.

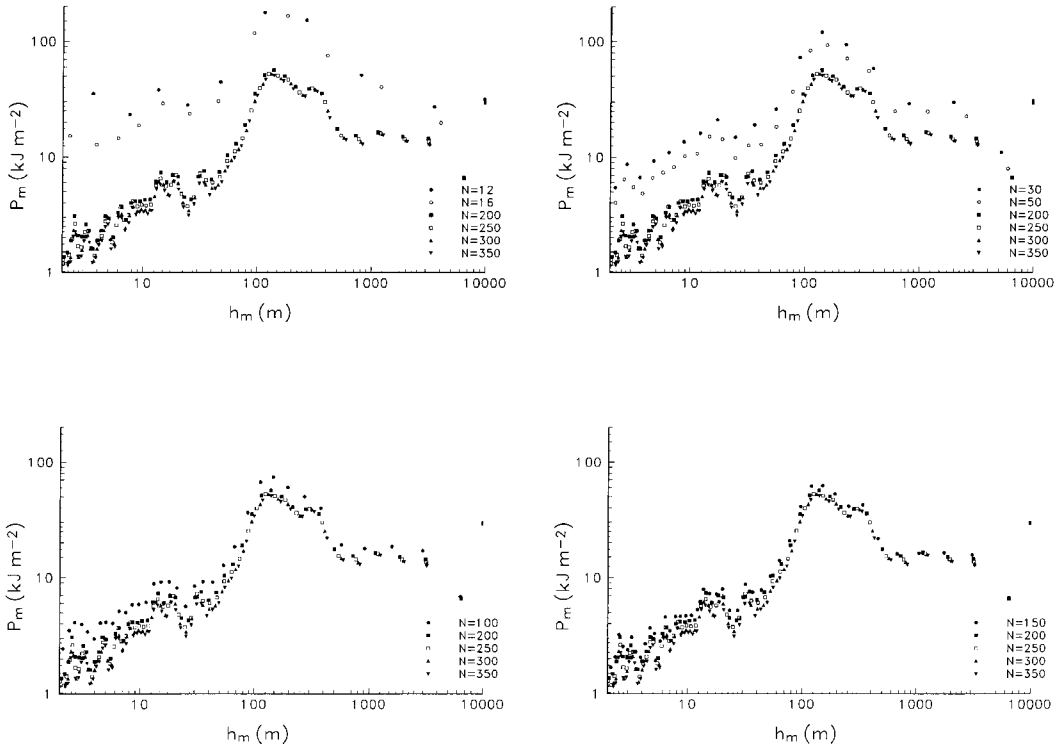

Fig. 5. As in Fig. 4, but with respect to eddy available potential energy.

numeric modes of low resolution spectra (i.e., calculated for smaller N) possess higher energy than the modes of more resolved spectra (i.e., calculated for larger N). However the total kinetic energy and the total available potential energy have approximately constant values for all spectra (Table 3). Neglecting the resolution differences, the available potential energy spectra present the same general features, with maxima and minima in the same vertical scales. This comment is also valid for the kinetic energy.

The results obtained in this section and in Section 3 put into evidence the little sensitivity of the vertical scale separation of the horizontal wind and mass fields to the number of Legendre polynomials, N, used in the construction of the vertical mode functions.

Such little sensitivity of the vertical scale decomposition of the general atmospheric circulation to the truncation order, together with the fact that as more terms are taken in the series of Legendre polynomials (12) more accurate numeric solutions will be obtained, raise the question of what must be the order of truncation of the series.

An answer may be given applying the same reasoning as in Section 3. In the present data set, the wind field is given at 12 standard pressure levels, and the boundary condition $\boldsymbol{V} = 0$ at the surface had been assumed. The geopotential field is given at the same 12 pressure levels. The data set also contains the sea level pressure which, through use of the hydrostatic equation, allows to compute the perturbed field of geopotential at the surface pressure level $p_s = 1010.5$ hPa. Therefore, since $\boldsymbol{V}$ and ϕ are known at 13 levels, the data must be projected at most onto 13 numeric vertical modes. Since the first 13 numeric vertical modes calculated with 16 Legendre polynomials adequately explain the vertical variances (kinetic energy and available potential energy, see Table 3) of the data, they should be regarded as an appropriate numerical base for the FGGE IIIb data set.

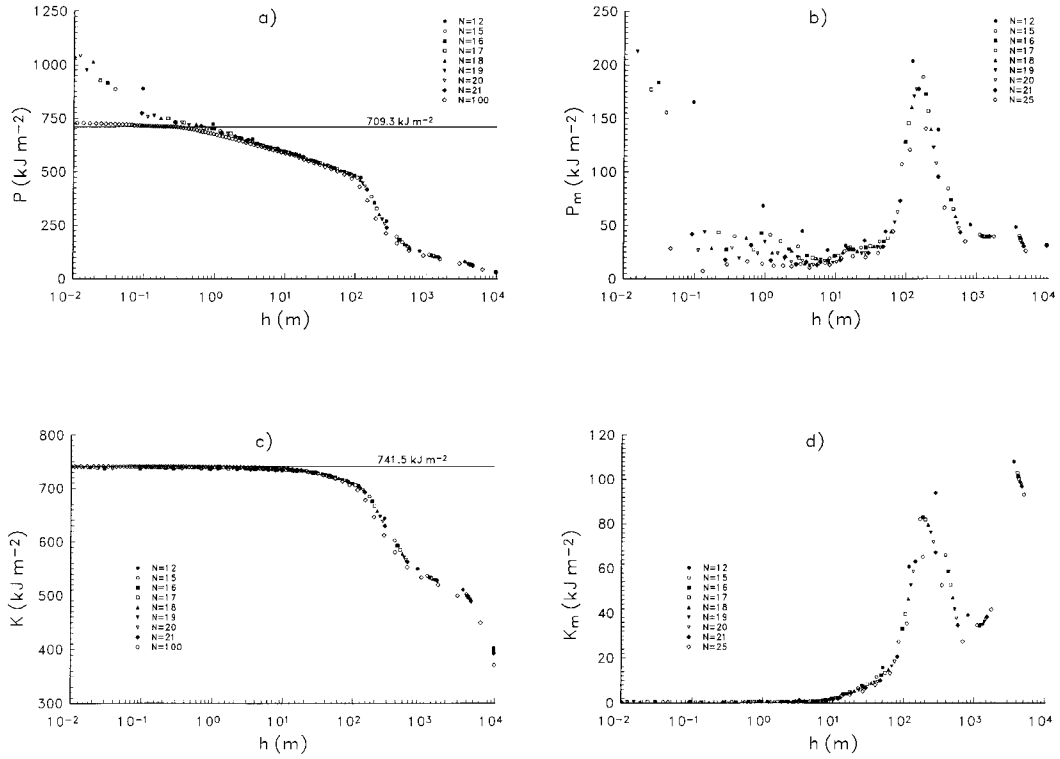

Fig. 6. Integrated energies for all modes with h greater than a given value (a, c) and vertical energy spectra (b, d) for the eddy available potential energy, P, and eddy kinetic energy, K.

4.2. NCEP re-analyses

The FGGE analyses possess only 12 vertical levels up to 30 hPa. In order to study the effects of the vertical resolution of the data set, calculations described in Subsection 4.1 were repeated for the NCEP re-analyses, which are available at 17 vertical levels: 1000, 925, 850, 700, 600, 500, 400, 300, 250, 200, 150, 100, 70, 50, 30, 20 and 10 hPa. Besides a greater resolution of the stratosphere, this data set presents two extra levels in the lower troposphere (925 hPa) and the middle troposphere (600 hPa).

The integrated values of the eddy available potential energy associated with modes of equivalent depths greater than a given value, for several truncation orders N, are presented in Fig. 6a, respective vertical energy spectra being shown in Fig. 6b. The horizontal lines in Figs. 6a,c represent the total energy calculated by direct data integration using eqs. (31) and (30), respectively. It may be observed that the integrated values are again independent of the truncation order, and that there is also a characteristic vertical available potential energy spectrum independent of the truncation order. In Fig. 6b, the spread at smaller equivalent depths is due to aliasing, and therefore such modes must be excluded from a numeric normal mode base.

Similar conclusions may be drawn in what concerns the eddy kinetic energy (Figs. 6c,d), with the exception of the aliasing that does not occur. It should be noted that the kinetic energy of the barotropic mode is not represented in Fig. 6d in order to make possible the use of a linear scale.

On the other hand, it must be stressed that (1) for $N = 12$, 15, 16 and 17 (lesser than the number of levels) the evolution of the spectra is similar to the cases $N = 18$, 19, 20 and 21 (greater than the number of levels); and that (2) in order to explain the vertical variance of the NCEP

re-analyses with only 18 vertical modes, the modes must be calculated with 21 Legendre polynomials.

5. Summary and conclusions

The VSE was numerically solved with a Galerkin method as used by Kasahara (1984). In order to assess the sensitivity of the vertical partition of energy (vertical energy spectrum) to the truncation order of the series of Legendre polynomials, several computational experiments were performed. First, following an heuristic procedure, the analytic case of an isothermal atmosphere with a rigid lid at the top $p_t \neq 0$ was considered. A simulated "data set" was projected onto the numeric modes of the isothermal atmosphere and compared with the projections onto the analytic modes. Then, following the procedure for the isothermal atmosphere, different numeric vertical normal mode bases were calculated for the FGGE atmosphere considering several truncation orders. The spectral distributions of kinetic and available potential energies in the vertical index domain, during the period 16–31 January 1979, were then calculated for the different numeric bases.

The main results of the computational experiments may be summarized as follows. There is a minimum equivalent depth such that varying the truncation order N of the Legendre polynomials series:

(1) the summation of the energies of numeric modes with equivalent depth greater or equal to the minimum depth, gives approximately constant values for the kinetic and available potential energies, i.e., considering a minimum value for the equivalent depth, the values of total kinetic and available potential energies present little sensitivity to the truncation order and are very near to the actual ones;

(2) neglecting resolution differences, the available potential energy spectra present the same general features with maxima and minima located at equivalent depths of the same order of magnitude; the same conclusion were obtained for the kinetic energy spectra.

With the aim of assessing the effect of the vertical resolution of the data set on the above results, the calculations were repeated for the NCEP re-analyses leading to the same conclusions.

Taking into account the above conclusions together with the fact that as more Legendre polynomials are considered in the series expansion, more accurate numeric solutions will be obtained, a rule must be established for the truncation order. The following procedure was adopted: if the data are available at M pressure levels, the numeric vertical modes must be calculated with a number N of Legendre polynomials such that only the first M modes are needed to explain all vertical variance of the data.

Finally, it is worth enphasizing that the calculation of the numeric base with a number of Legendre polynomials N greater than the number of levels eliminates the problem of aliasing in the higher internal modes.

6. Acknowledgements

This study was partly supported by the PRODEP program N.3/PRODEP/94/5/Action 5.2 and the project PRAXIS 3/3.2/EMG/1949/95.

REFERENCES

Daley, R. 1978. The application of non-linear normal mode initialization to an operational forecast model. *Rev. Atmos.-Ocean* **17**, 97–124.

Daley, R. 1991. *Atmospheric data analysis*. Cambridge University Press.

Fulton, S. R. and Schubert, W. H. 1985. Vertical normal mode transforms: theory and application. *Mon. Wea. Rev.* **113**, 647–658.

Kasahara, A. and Puri, K. 1981. Spectral representation of three-dimensional global data by expansion in normal mode functions. *Mon. Wea. Rev.* **109**, 37–51.

Kasahara, A. 1984. The linear response of a stratified global atmosphere to tropical thermal forcing. *J. Atmos. Sci.* **41**, 2217–2237.

Kung, E. C. and Tanaka, H. 1983. Energetics analysis of the global circulation during the Special Observation Periods of FGGE. *J. Atmos. Sci.* **40**, 2575–2592.

Murakami, T. 1967. Vertical transfer of energy due to stationary disturbances induced by topography and diabatic heat sources and sinks. *J. Meteor. Soc. Japan* **45**, 205–231.

Sasaki, Y. K. and Chang, L. P. 1985. Numerical solution

of the vertical structure equation in the normal mode method. *Mon. Wea. Rev.* **113**, 782–793.

Staniforth, A., Béland, M. and Côté, J. 1985. An analysis of the vertical structure equation in sigma coordinates. *Atmos.-Ocean* **23**, 323–358.

Tanaka, H. 1985. Global energetics analysis by expansion into three-dimensional normal mode functions during the FGGE winter. *J. Meteor. Soc. Japan* **63**, 180–200.

Tanaka, H. Kung, E. C. 1988. Normal mode energetics of the general circulation during the FGGE Year. *J. Atmos. Sci.* **45**, 3723–3736.

Tanaka, H. and Kung, E. C. 1989. A study of low-frequency unstable planetary waves in realistic zonal and zonal varying basic states. *Tellus* **41A**, 179–199.